Jurnal
Teknologi

Full paper

Bio-Based Lubricants for Numerical Solution of Elastohydrodynamic Lubrication

Dedi Rosa Putra Cupu[a], Jamaluddin Md Sheriff[b], Kahar Osman[b*]

[a]Mechanical Engineering Dept. of Engineering Faculty, University of Riau, Pekanbaru, Riau, Indonesia
[b]Faculty of Mechanical Engineering, Universiti Teknologi Malaysia, Skudai, Malaysia

*Corresponding author: kahar@fkm.utm.my

Article history

Received :15 June 2012
Received in revised form :12 August 2012
Accepted :28 August 2012

Graphical abstract

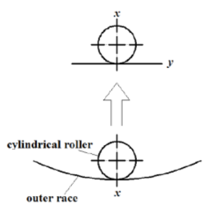

Abstract

This paper presents a numerical solution of elastohydrodynamic lubrication (EHL) problem in line contacts which is modeled through an infinite cylinder on a plane to represent the application of cylindrical roller bearing. In this work, the contact between roller element and raceway of outer ring of the cylindrical roller bearing is simulated using vegetable oils as bio-based lubricants. Temperature is assumed to be constant at 40oC. The results show that the EHL pressure for all vegetable oils was increasing from inlet flow until the center, then decrease a bit and rise to the peak pressure. The shapes of EHL film thickness for all tested vegetable oils are almost flat at contact region.

Keywords: Bio-based lubricant, vegetable oil, elastohydrodynamic lubrication

1.0 INTRODUCTION

Environmentally acceptable should be considered as the most important thing in industrial and transportation application including their lubrication system. Leakages, spills and disposal of lubricants will cause the pollution and the environment health (Erhan et. al., 2006) because 5-10 million tons of petroleum based oleochemical enter the biosphere every year (Gawrilow, 2003) which derived from the food industry, petroleum products, and by products such as lubricants hydraulic and cutting oils. Based on the market overview (Bremmer and Plonsker, 2008) total lubricant demand in 2007 was about 41.8 million metric tons, the growth of lubricant demand was expected to be about 2% per year through 2010. Sales of all lubricants in the United States of America were in the range of 2.5 billion gallons in 2006. This high demand on lubricant needs the renewable resources to avoid the crisis energy. Due to this energy crisis and pollution of the environment, bio-based oils are possible to be used as industrial lubricating oils, instead of petroleum-based oils such as mineral oils and synthetic oils.

Bio-based oils are found in the seed or fruit of various plants or animals, vegetable oils are one of these bio-based oils where are manufactured from the plants. Vegetable oils consist of triglycerides, which are glycerol molecules with three long chains of fatty acids attached at the hydroxyl group by ester linkages. These fatty acids have similar length, between 14 and 22 carbons long with varying levels of unsaturation. Long and polar fatty acids will interact strongly with metallic surfaces, reducing friction and wear, and providing more stable viscosity, or high viscosity index (Fox and Stachowiak, 2007). Unfortunately, these unsaturated double bonds of fatty acids in vegetable oils are also active for many reactions, including oxidation, lowering their consistence to oxidative degradation and poor low-temperature properties. Another disadvantage of using vegetable oil as a lubricant is only small range of viscosities is available due to the similarity in vegetable oil structure. However, these concerns have been improved by many researchers. Quinchia *et al.* (2010) have successfully modified the viscosity of vegetable oils, such as soybean oil, sunflower oil and castor oil, by using Ethylene-Vinyl Acetate copolymer (EVA) as additive material. Erhan and Asadauskas (2000) have chemically modified the triglycerides of vegetable oils (soybean oil and high oleic sunflower oil) to eliminate their polyunsaturation for better oxidative stability, and improved their low temperature properties.

Recently, some vegetable oils are widely being used as the alternative base oil for lubricants in the world. Many researchers have investigated to use vegetable oils as lubricants. Syahrullail *et al*. (2011) have used Refined, Bleached and Deodorized (RBD) palm stearin, which one of the refined palm oil types, as the lubricant in a cold work forward plane strain extrusion process. This RBD palm oil has also been investigated by Kadir *et al.* (2010) to find the friction coefficient of RBD palm oil and this oil has a potential for automatic transmission lubricant. Assessment of tribological properties, such as wear and friction, for palm oil has been compared to mineral oil using universal wear and friction machine and a two-stroke engine, and the vegetable oil is better performance in terms of wear (Masjuki et. al., 1999). Mia and Ohno (2010) have investigated the high pressure physical properties, rheological behavior and phase diagram of mustard oil and coconut oil, which results showed that mustard and coconut oil could be used as lubricants.

In this research, vegetable oils which have been tested by Mia and Ohno (2010), as shown in Table 1, will be used as the lubricants in simulation of elastohydrodynamic lubrication, which the contact zone of this lubrication is too small so that the high pressure on the contacting elements will deform the surfaces, such as contact between mating-gears, roller element bearing, cams, etc. In this simulation, cylindrical roller element bearing will be used as physical modeling which is a device used to support a rotating shaft to the bearing housing and reduce the friction between the cylindrical roller element and the raceway of outer ring, as shown in Figure 1. As the limitation study is in only one dimensional, a simple assumption for the width of the bearing is effectively infinite and the pressure distribution is uniform in the *y* direction, meaning side leakage is neglected. Another assumption is simulation running in constant temperature (isothermal condition). Calculation of film thicknesses and pressures in line contact of elastohydrodynamic lubrication is based on the fast and accurate method, developed by Houpert and Hamrock (1986), which used Newton-Raphson method in solving the elasticity and Reynolds equation simultaneously. The advantage of this method is that solutions can be obtained for no load limitations and solved in a small amount of iterations with small number of computer running time. Effects of sliding ratio of velocity on the elastohydrodynamic pressure and film thickness profiles will also be investigated.

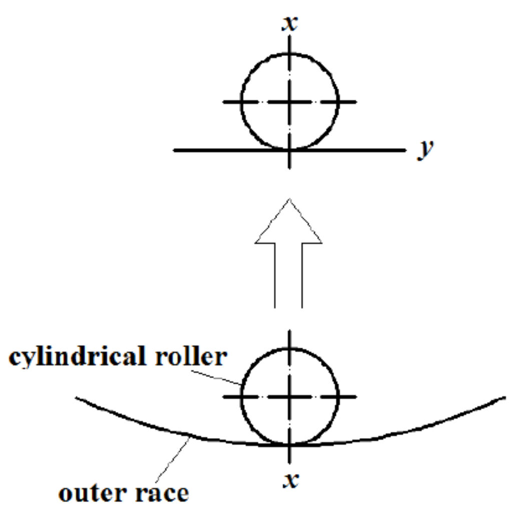

Figure 1 Cylindrical roller element bearing for physical modeling of simulation

Table 1 Physical properties of tested oils (Mia and Ohno, 2010)

Oil name	**Density, ρ (g/cm^3) at 15ºC**	**Kinematic viscosity, ν (mm^2/s) at 40ºC**	**Pressure-viscosity coefficient, α (GPa^{-1})**
Mustard oil	0.9180	44.1	9.46
Coconut oil	0.9260	27.6	13.09
Mineral oil	0.8663	28.6	12.65

2.0 EQUATIONS

All equations in this simulation are made in dimensionless using Hertzian dry contact. For two-dimensional flow, isothermal and steady state condition, the dimensionless Reynolds equation can be written as:

$$f_i = H_i^3\left(\frac{dP}{dX}\right)_i - K\bar{\eta}_i\left(H_i - \frac{\bar{\rho}_e H_e}{\bar{\rho}_i}\right) = 0 \qquad \text{(a)}$$

All dimensionless parameters are detailed in the nomenclature.

$$K = \frac{3}{4}\pi^2\frac{U}{W^2} \qquad \text{(b)}$$

H_i is the dimensionless film thickness, calculated with:

$$H_i = H_0 + \frac{X_i^2}{2} + \sum_{j=1}^{N} D_{ij}P_{ij} \qquad \text{(c)}$$

Dimensionless lubricant density ($\bar{\rho}_i$) is assumed to depend on the pressure only according to Dowson and Higginson [12].

$$\bar{\rho}_i = 1 + \frac{0.6\times10^{-9}\,p_H P_i}{1+1.7\times10^{-9}\,p_H P_i} \qquad \text{(d)}$$

For calculation of viscosity, Roelands' relationship of viscosity-pressure is employed in this simulation.

$$\bar{\eta}_i = \exp\left\{\left[\ln(\eta_0)+9.67\right]\left(-1+\left(1+5.1\times10^{-9}\,p_H P_i\right)^Z\right)\right\} \qquad \text{(e)}$$

where, $$Z = \frac{\alpha}{\left(\ln(\eta_0)+9.67\right)\left(5.1\times10^{-9}\right)} \qquad \text{(f)}$$

The dimensionless load balance equation is expressed as:

$$\int_{X_{in}}^{X_{out}} P\,dX = \frac{\pi}{2} \qquad \text{(g)}$$

The unknowns in this problem are:

- X_{end} - outlet boundary
- N - number of nodes
- H_0 - central film thickness
- $\rho_e H_e$ value of density times film thickness, ρH where $dP/dX = 0$
- P_j - pressure at node j (j = 2, N)

The boundary conditions are $P_1 = 0$ for $X_1 = X_{min}$ and $P = dP/dX$ for $X = X_{end}$.

3.0 NUMERICAL SOLUTION

Newton-Raphson formula will be used in order to solve the non-linear of Reynolds equation. From Figure 2, to find a root where $f(x) = 0$ and x_i is initial guess of root, as well known that the first differential of $f(x)$ can be written as:

$$f'(x)=\tan\theta=\frac{f(x_i)-0}{x_i-x_{i+1}} \tag{h}$$

Equation (9) can be rewritten as:

$$-f(x_i)=(\Delta x_i)\,f'(x_i) \tag{i}$$

where

$$\Delta x_i = x_{i+1}-x_i \tag{j}$$

Using this concept of Newton-Raphson, the unknowns $\overline{\rho}_e H_e$, P_j, and H_0 can be calculated as:

$$\left(\overline{\rho}_e H_e\right)^{new}=\left(\overline{\rho}_e H_e\right)^{old}+\left[\Delta\left(\overline{\rho}_e H_e\right)\right]^{new} \tag{k}$$

$$P_j^{\,new}=P_j^{\,old}+\left(P_j\right)^{new} \tag{l}$$

$$H_0^{\,new}=H_0^{\,old}+\left(H_0\right)^{new} \tag{m}$$

We have for each node i of equation (3) is:

$$\left[\frac{\partial f_i}{\partial\left(\overline{\rho}_e H_e\right)}\right]^{old}\left[\Delta\left(\overline{\rho}_e H_e\right)\right]^{new}+\sum\left(\frac{\partial f_i}{\partial P_j}\right)^{old}\left(\Delta P_j\right)^{new}+\left(\frac{\partial f_i}{\partial H_0}\right)^{old}\left(\Delta H_0\right)^{new}=f_i^{old} \tag{n}$$

The constant load is:

$$\int_{X_{\min}}^{X_{end}}\left(\Delta P\right)^{new}dX=\frac{\pi}{2}-\int_{X_{\min}}^{X_{end}}P^{old}dX=\left(\Delta W\right)^{new} \tag{o}$$

or

$$\sum_{j=2}^{N}C_j\left(\Delta P_j\right)^{new}=\left(\Delta W\right)^{new} \tag{p}$$

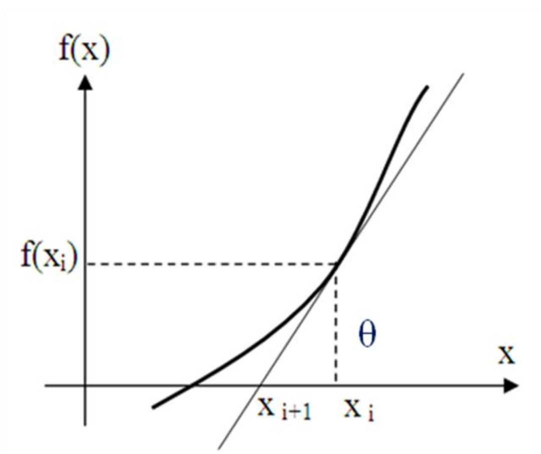

Figure 2 Root finding of Newton-Raphson method

4.0 RESULTS AND DISCUSSION

Elastohydrodynamic lubrication parameters, such as pressure profiles and film thicknesses for coconut oil and mustard oil have been simulated for rolling element bearing application. Temperature was assumed constant at 40°C and speed of bearing was assumed in steady state. Dimensionless load and dimensionless speed were set identical to the running simulation by Houpert and Hamrock (1986), W = 2.0452 x 10^{-5} and U = 1.0 x 10^{-11}. The maximum number of nodes was fixed at 321. The X_{in} and X_{out} were set at -4 and 1.5 respectively. Hertzian pressure and thickness profile were used as initial condition. Roelands' relationship of pressure-viscosity was used because of its high load running capability. For comparison, mineral oil of P150 was used in running this simulation. Figures 3 to 5 show the pressures profile and film thicknesses for all tested oils. It should be noted that the x axis in all graphs indicated the dimensionless distance from the centre of component of roller bearing where the lubricant enters the contacted components from the left side of the two elements. This dimensionless distance was obtained by dividing the distance along rolling direction (x) with the half Hertzian length (b), as shown in Figure 1.

Pressure profile and film thickness for coconut oil are depicted in Figure 3. The pressure of elastohydrodynamic lubrication increased from the inlet flow (X = 4) and reach the maximum pressure at the center of roller. This increasing plot followed the Hertzian pressure profile, but in this profile, there was a second local maximum located near the outlet, referred to as the "pressure spike", with the maximum pressure was $P_{\max}$ = 0.96527. After reaching the second peak position, the pressure dropped sharply to the outlet flow (X_{end} = 1.16153), as shown Figure 3 (a). The film thickness shape for coconut oil is shown in Figure 3 (b). Initial guess for dimensionless central film thickness was H_0 = 0.6. The film thickness shape of elastohydrodynamic lubrication for coconut oil decreased from the inlet flow until reached the contacted zone and almost flat at this contacted area (from X = -1 to X = 1). There was a valley shape was formed at the end of contacted zone due to the spike of elastohydrodynamic pressure, $H_{\min}$ = 0.30683. Figure 3 (c) shows the blowup of the elastohydrodynamic pressure and film thickness for coconut oil in the contacted zone. In this figure, it can be seen that the value of film thickness was almost two orders of magnitude from the Hertzian film thickness.

Pressure spike for mustard oil was smaller than pressure spike of coconut oil, located near to the maximum Hertzian pressure while spike of mineral oil was almost coincident with coconut oil (Figure 4 (a)). It was caused by the solidification temperature of coconut oil was higher than mustard oil which affected to the pressure-viscosity coefficient, while the pressure viscosity coefficient of coconut oil was almost same as mineral oil (P150N) but it was lower than in case of mustard oil (Mia and Ohno, 2010). Pressure spike of mustard oil and mineral oil are $P_{\max}$ = 0.954322 and $P_{\max}$ = 0.95826, respectively. This case applied to the film thickness also, as shown in Figure 4 (b), while the thickness of coconut oil was almost coincident with mineral oil and higher than mustard oil's thickness. The minimum film thickness for mustard oil is $H_{\min}$ = 0.26383 and mineral oil is $H_{\min}$ = 0.30171. Detail pressure profiles and film thicknesses at the contacted zone can be seen at Figure 4 (c).

The effects of sliding ratio on the elastohydrodynamic parameters have been investigated and shown in Figure 5. This simulation was running for coconut oil and the dimensionless load was set fixed as W = 2.0452 x 10^{-5} and the velocity of upper roller was set as v_a = 1.04542 m/s. It should be noted that the dimensionless load was obtained by dividing the applied load per unit length (w) with the multiplying of equivalent Young's modulus (E') and the equivalent radius of contact (R), as described in nomenclature. Figure 5 shows that the value and position of pressure spike and film thickness differ for all effects of sliding ratio. Higher ratio cause lower pressure spike and lower minimum film thickness and the location are closer to the outlet zone.

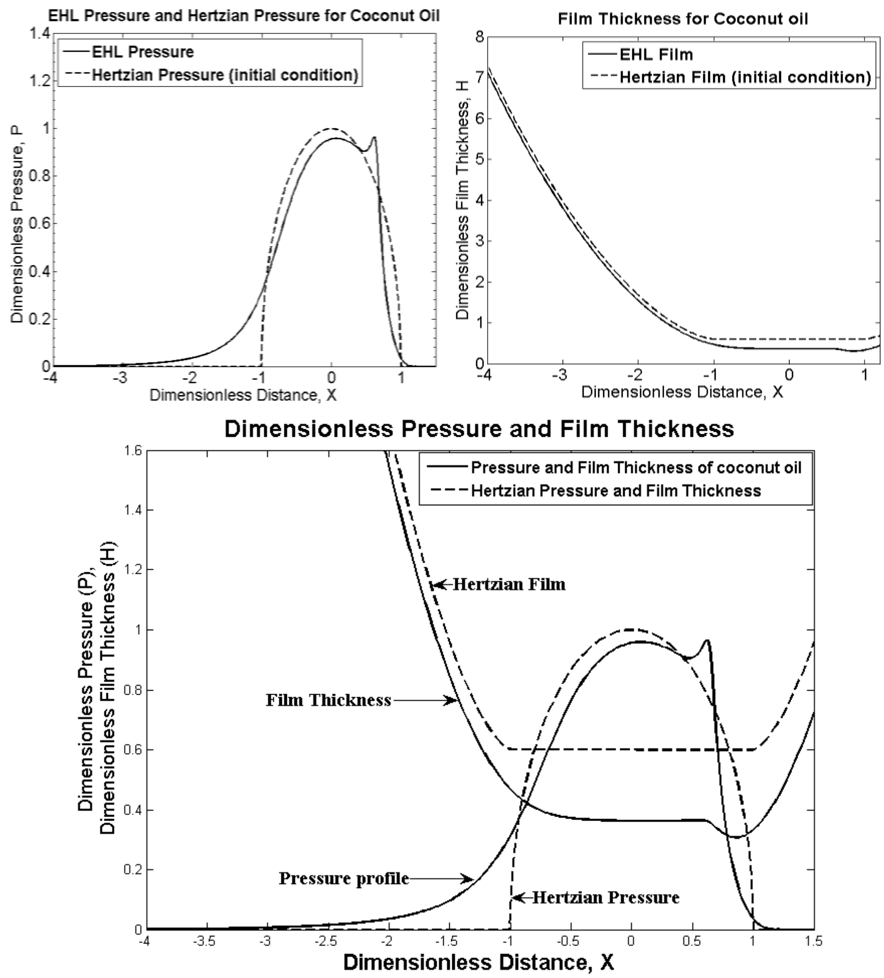

Figure 3 Pressure profile and film thickness shape using coconut oil as the lubricant; $W = 2.0452 \times 10^{-5}$; $U = 1.0 \times 10^{-11}$

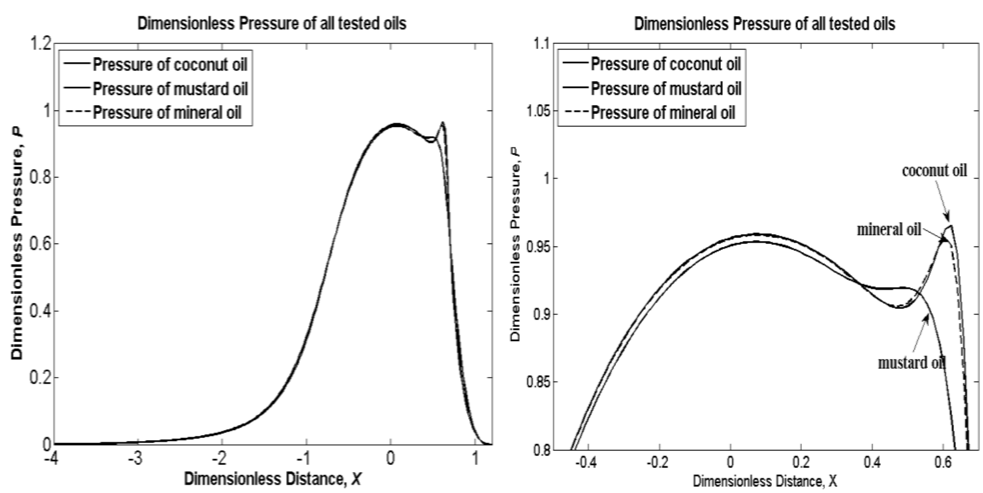

(a) (b)

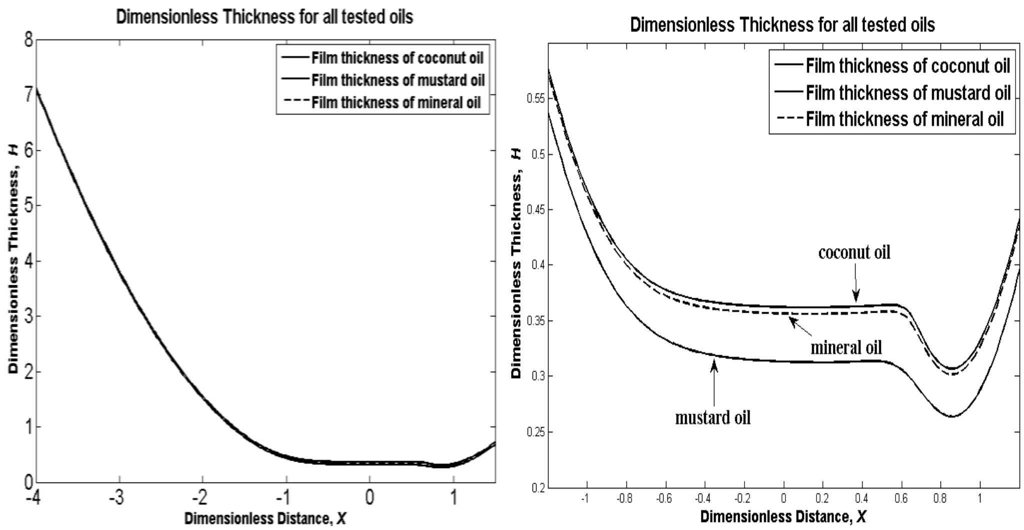

(c) (d)

Figure 4 Pressure profile and film thickness shape for all tested oils; $W = 2.0452 \times 10^{-5}$; $U = 1.0 \times 10^{-11}$. (*a*). Dimensionless pressure profile. (*b*). Blowup dimensionless pressure profile at the contact area. (*c*). Dimensionless film thickness distribution. (*d*). Blowup dimensionless film thickness distribution at the contacted zone

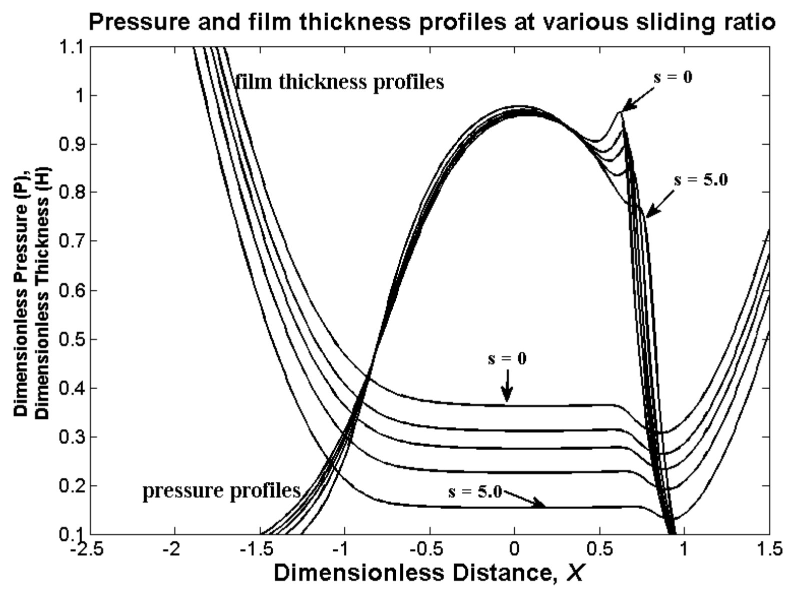

(*a*)

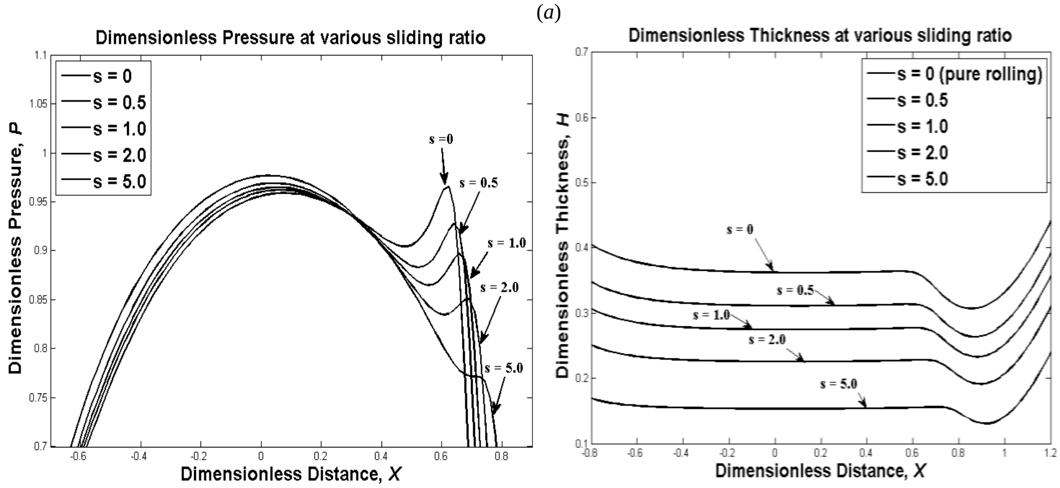

(b) (c)

Figure 5 Effect of sliding ratio on the elastohydrodynamic parameters. (*a*). Pressure and film thickness at various sliding ratio. (*b*). Blowup pressure profiles at the contact area. (*c*). Blowup film thickness distribution at the contact area

4.0 CONCLUSION

Coconut oil and mustard oil have been simulated as lubricants in order to obtain the elastohydrodynamic parameters by using a fast and accurate approach of Houpert and Hamrock. For comparison, mineral oil of P150N has been used to see the possibility to substitute it with vegetable oils. All simulated oils data were obtained from experiment of Mia and Ohno. The conclusion can be drawn that coconut oil has similar pressure profile and film thickness shape with the mineral oil and mustard oil has lower values than mineral oil. However, these vegetable oils have a potential to substitute the function of mineral oil as lubricant using in roller element bearing application to reduce crisis energy.

Acknowledgement

The authors acknowledge to thanks to Research Management Centre (RMC) of Universiti Teknologi Malaysia (UTM) for their funding to this research.

Nomenclature

b = Half Hertzian length, $R\sqrt{8W/\pi}$, m
Cj = weighting factors used to integrated **P**
E = Young's modulus of surface, Pa
E' = Equivalent Young's modulus,

$$\frac{1}{E'} = \frac{1}{2}\left(\frac{1-\nu_a^2}{E_a} + \frac{1-\nu_b^2}{E_b}\right), \text{ Pa}$$

G = material parameter, $\alpha E'$
H = dimensionless film thickness, hR/b^2
H_e = dimensionless film thickness where $dP/dX = 0$
H_0 = dimensionless constant used in calculation of H
h = film thickness, m
i, j = nodes
N = number of nodes used in linear system
N_{max} = maximum number of nodes used in mesh
P = dimensionless pressure, p/p_H, Pa
P_s = dimensionless pressure at spike
p_H = maximum Hertzian pressure, $E'b/4R$, Pa
R = equivalent radius of contact, m
U = dimensionless speed parameter, $\eta_0 u/E'R$
u = average entrainment rolling speed, $(u_a + u_b)/2$, m/s.
W = dimensionless load parameter, $w/E'R$
w = applied load per unit length, N/m
X = dimensionless abscissa, x/b
X_{end} = outlet distance
X_{max} = maximum value of X in mesh
X_{min} = minimum value of X in mesh, X_1
x = abscissa along rolling direction, m
Z = Roelands parameter
α = pressure-viscosity coefficient, m^2/N
η_0 = viscosity at operating temperature and ambient pressure, N s/m^2
ν = Poisson's ratio
$\bar{\rho}$ = relative density
$\bar{\rho}_e$ = relative density where $H = H_e$

Subscripts

a = surface a
b = surface b
H = Hertz
i = at node number i
j = at node number j
max = maximum value
min = minimum value

References

[1] Erhan, S. Z., Adhvaryu, A., Sharma, B. K. 2006. Chemically Functionalized Vegetable Oils. In: Rudnick, L. R. (Eds). Synthetics, Mineral Oils, and Bio-Based Lubricants. *Chemistry and Technology*. Boca Raton: Taylor and Francis Group.
[2] Gawrilow, I. 2003. Palm Oil Usage in Lubricants. Presented at 3rd Global Oils and Fats Business Forum USA. Interfacing with the Global Oils and Fats Business.1–19.
[3] Bremmer, B. J., Plonsker, L. 2008. Bio-Based Lubricants. A Market Opportunity Study Update, Prepared for the United Soybean Board: Omni Tech International, Ltd. 1–31.
[4] Fox, N. J., and Stachowiak, G. W. 2007. Vegetable Oil-based Lubricants–A Review Oxidation. *Tribology International*. 40: 1034–1046.
[5] Quinchia, L. A., Delgado, M. A., Valencia, C., Franco, J. M., Gallegos, C. 2010. Viscosity Modification of Different Vegetable Oils with EVA Copolymer for Lubricant Applications. *Industrial Crops and Products*. 32: 607–612.
[6] Erhan, S. Z., Asadauskas, S. 2000. Lubricant basestocks from Vegetable Oils. *Industrial Crops and Products*. 11: 277–282.
[7] Syahrullail, S., Zubil, B. M., Azwadi, C. S. N., Ridzuan, M. J. M. 2011. Experimental Evaluation of Palm Oil as Lubricant in Cold Forward Extrusion Process. *International Journal of Mechanical Sciences*. 53: 549–555.
[8] Kadir, K. A., Ing, T. C., Tawi, K. B., Samion, S., and Supriyo, B., 2010. Investigation of Friction Characteristics of Refined, Bleached, and Deodorized Palm Olein Compared with Automatic Transmission Fluid Lubricant. Proceedings of 3rd International Meeting of Advances in Thermofluids, Singapore.84–89.
[9] Masjuki, H. H., Maleque, M. A., Kubo, A., Nonaka, T. 1999. Palm Oil And Mineral Oil Based Lubricants–Their Tribological and Emission Performance. *Tribology International*. 32: 305–314.
[10] Mia, S., Ohno, N. 2010. Prospect of Mustard Oil and Coconut Oil as Environment Friendly Lubricant for Bangladesh. Proceedings of International Conference on Environmental Aspects of Bangladesh, Japan. 120-121.
[11] Houpert, L. G., Hamrock, B. J. 1986. Fast Approach for Calculating Film Thicknesses and Pressures in Elastohydrodynamically Lubricated Contacts at High Loads. *ASME Journal of Tribology*. 108:411–420.